Available online at http://jprm.sms.edu.pk/
Journal of Prime Research in Mathematics, 21(1) (2025), 101-118

Journal of Prime Research in Mathematics

Modeling Hepatitis C with Piecewise Derivatives: Comparative Insights from Deterministic and Stochastic Frameworks

Ipek Korkmaz[a], Seda Igret Araz[a,*]

[a]*Department of Mathematics Education, Faculty of Education, Siirt University, Siirt 56100, Turkey*

Abstract

In this paper, we conduct a comprehensive investigation of deterministic–stochastic modeling approaches for Hepatitis C using piecewise fractional operator techniques. This novel framework captures a wide range of dynamic behaviors, from deterministic transitions to stochastic fluctuations. By constructing piecewise differential operators that switch between deterministic and stochastic regimes, we demonstrate the innovative potential of this methodology. To validate its effectiveness, we present graphical simulations of the proposed model. The results show that these operators offer a more flexible and accurate representation of the complex dynamics characteristic of real-world systems. By effectively capturing distinct behaviors over different time intervals, this approach opens new avenues for research across multiple scientific disciplines.

Keywords: Hepatit-C model, piecewise derivative, stochastic approaches, existence and uniqueness.

1. Introduction

The recognition of a novel form of hepatitis emerged in the late 1970s,following reports of hepatitis cases linked to blood transfusions. Upon investigation, it was determined that the causative agent was neither Hepatitis A (HAV) nor Hepatitis B (HBV), the two known hepatotropic virusesn at the time. As a result, the unidentified pathogen was provisionally termed non-A, non-B hepatitis. Continued research eventually led to the identification of this virus in 1989 as the Hepatitis C virus (HCV) [1–5]. HCV is a hepatotropic virus that specifically targets hepatocytes—the primary functional cells of the liver—causing hepatic inflammation and infection. The clinical presentation of Hepatitis C is often asymptomatic or marked by nonspecific symptoms, allowing the disease to progress undetected in many individuals. It is estimated that approximately 80% of acute HCV infections become chronic [1–6], which can lead to serious liver conditions such as fibrosis, cirrhosis, and hepatocellular carcinoma. Globally, around 1% of the population is estimated to be chronically infected with HCV [3,7,8]. One of the primary transmission routes for HCV

*Corresponding author
Email addresses: ipekkrkmz7@hotmail.com (Ipek Korkmaz), sedaaraz@siirt.edu.tr (Seda Igret Araz)

Received : 27 July 2025*; Accepted:* 20 September 2025*; Published Online:* 22 September 2025.

is exposure to contaminated blood products, particularly via parenteral means. Despite improvements in screening and safety protocols, intravenous drug use and needle sharing remain significant contributors to HCV transmission [9].

To better understand HCV transmission dynamics and evaluate treatment strategies, various mathematical models have been developed [10–17]. For example, Pitcher et al. [11] conducted a comprehensive review of modeling studies focused on HCV transmission and prevention among people who inject drugs (PWID). Their work highlights the mathematical frameworks employed and how such models can inform strategies to meet the World Health Organization's (WHO) elimination goals. In a different context, Dahari et al. [12] proposed a model describing the intracellular replication dynamics of subgenomic HCV RNA within Huh-7 cells, from initial transfection to the steady-state phase. This model provides valuable insights into replication mechanisms and supports the development of antiviral therapies. Additional contributions to HCV modeling include the work of Vujovic et al. [17], who analyzed the stability properties of two stochastic models incorporating isolation stages. They established the existence and uniqueness of global positive solutions, supported by numerical simulations. Similarly, Lestari et al. [18] addressed optimal control problems within a stochastic differential equation framework, aiming to minimize side effects by using control variables to represent pharmacological interventions targeting infection prevention and viral production. In a related study [19], Lestari and colleagues examined the qualitative behavior of a stochastic epidemic model of HCV at the cellular level. Methodological insights into stochastic modeling are provided in [20], where the authors derive exact solutions for stochastic differential equations using Itô calculus, discuss parameter estimation strategies, and compare various methods with illustrative examples.

An advanced mathematical framework increasingly applied in infectious disease modeling is fractional calculus, which extends classical differentiation and integration to non-integer (fractional) orders. The origins of fractional calculus trace back to a 1695 correspondence between Leibniz and L'Hôpital about the concept of derivatives of arbitrary order. Over time, multiple formal definitions have emerged, including the Riemann–Liouville [22], Caputo [21], Caputo–Fabrizio [24], and Atangana–Baleanu [25] formulations. These differ primarily in their kernel functions, such as power-law, exponential decay, or Mittag–Leffler functions. More recently, Atangana and Araz [26] introduced the concept of piecewise differential operators [28], offering a flexible and practical tool for modeling complex systems, particularly those involving transitions between deterministic and stochastic behaviors [27]. This framework has opened new avenues for the theoretical modeling of dynamic systems, including viral infections such as HCV.

In this study, we not only conduct deterministic and stochastic analyses for the Hepatitis C virus (HCV), but also aim to simulate the model introduced in [19] under deterministic-stochastic or stochastic-deterministic transitions by employing the piecewise derivative approach, which has the potential to unify these two processes within a single framework. In doing so, a more flexible and realistic modeling structure is proposed, one that simultaneously captures both randomness and memory effects, as frequently observed in real biological systems. To numerically solve such a complex and multi-component system, we present a numerical method based on Newton polynomial interpolation [23], which offers significant advantages in terms of both accuracy and computational efficiency in solving the associated model.

This study is organized as follows: Section 2 presents the necessary definitions of fractional and piecewise differential operators that form the mathematical foundation of the models. Section 3 formulates the deterministic Hepatitis C model, including analysis of equilibrium points, positivity of solutions, and derivation of the reproductive number. Section 4 extends the model to include stochastic effects, presenting the stochastic Hepatitis C model along with results on the existence and uniqueness of solutions. Section 5 explores the piecewise Hepatitis C model under various scenarios, incorporating classical, fractional, and stochastic derivatives. We discuss both deterministic and hybrid deterministic-stochastic settings using different fractional operators. Section 6 summarizes the main findings and discusses the results of numerical simulations.

2. Definitions of fractional and piecewise differential operators

In this section, several fractional and piecewise differential operators, chosen from among the various types introduced in the literature, are presented [26]. These operators are the ones we intend to utilize in our analysis. The research in [26] provides a comprehensive framework for piecewise differential operators, and here, we focus specifically on those that are most relevant to our modeling approach.

Definition 1. Let $\kappa(\varsigma)$ be differentiable function. The piecewise derivative is defined by

$$ {}_0^{PC}D_\varsigma^\zeta \kappa(\varsigma) = \begin{cases} \kappa'(\varsigma) \text{ if } 0 \le \varsigma \le \varsigma_1 \\ {}_{\varsigma_1}^{C}D_\varsigma^\zeta \kappa(\varsigma) \text{ if } \varsigma_1 \le \varsigma \le T \end{cases}, \tag{2.1} $$

where ${}_0^{PC}D_\varsigma^\zeta$ represents the classical derivative on $0 \le \varsigma \le \varsigma_1$ and derivative with power-law kernel on $\varsigma_1 \le \varsigma \le T$. Here, the fractional derivative with power-law kernel of the function $\kappa(\varsigma) \in H^1(0,T)$ is defined by

$$ {}_0^{C}D_\varsigma^\zeta \kappa(\varsigma) = \frac{1}{\Gamma(1-\zeta)} \int_0^\varsigma \kappa'(\zeta)(\varsigma-\zeta)^{-\zeta} d\zeta, $$

where $0 < \zeta \le 1$.

Definition 2. The piecewise integral of $\kappa(\varsigma)$ with respect to ς is given as

$$ {}^{PC}I_\varsigma \kappa(\varsigma) = \begin{cases} \int_0^\varsigma \kappa(\sigma) d\sigma \text{ if } 0 \le \varsigma \le \varsigma_1 \\ \frac{1}{\Gamma(\zeta)} \int_{\varsigma_1}^\varsigma \kappa(\sigma)(\varsigma-\sigma)^{\zeta-1} d\sigma \text{ if } \varsigma_1 \le \varsigma \le T \end{cases}, \tag{2.2} $$

where ${}^{PC}I_\varsigma$ denotes the classical integral on $0 \le \varsigma \le \varsigma_1$ and the associated integral on $\varsigma_1 \le \varsigma \le T$. The associated fractional integral is denoted as:

$$ {}_0^{PL}J_\varsigma^\zeta \kappa(\varsigma) = \frac{1}{\Gamma(\zeta)} \int_0^\varsigma \kappa(\zeta)(\varsigma-\zeta)^{\zeta-1} d\zeta. $$

Definition 3. Let $\kappa(\varsigma)$ be differentiable function. The piecewise derivative [26] is defined by

$$ {}_0^{PCF}D_\varsigma^\zeta \kappa(\varsigma) = \begin{cases} \kappa'(\varsigma) \text{ if } 0 \le \varsigma \le \varsigma_1 \\ {}_{\varsigma_1}^{CF}D_\varsigma^\zeta \kappa(\varsigma) \text{ if } \varsigma_1 \le \varsigma \le T \end{cases}, \tag{2.3} $$

where ${}_0^{PCF}D_\varsigma^\zeta$ denotes the classical derivative on $0 \le \varsigma \le \varsigma_1$ and derivative with power-law kernel on $\varsigma_1 \le \varsigma \le T$. Here, the fractional derivative with exponential decay kernel [24] of the function $\kappa(\varsigma) \in H^1(0,\varsigma)$ is formulated as:

$$ {}_0^{CF}D_\varsigma^\zeta \kappa(\varsigma) = \frac{1}{1-\zeta} \int_0^\varsigma \kappa'(\zeta) \left[-\frac{\zeta}{1-\zeta}(\varsigma-\zeta) \right] d\zeta, $$

where $0 < \zeta \le 1$.

Definition 4. The piecewise integral of $\kappa(\varsigma)$ with respect to ς is given as

$$ {}^{PCF}I_\varsigma \kappa(\varsigma) = \begin{cases} \int_0^\varsigma \kappa(\sigma) d\sigma \text{ if } 0 \le \varsigma \le \varsigma_1 \\ (1-\zeta)\kappa(\varsigma) + \zeta \int_{\varsigma_1}^\varsigma \kappa(\sigma) d\sigma \text{ if } \varsigma_1 \le \varsigma \le T \end{cases}, \tag{2.4} $$

where ${}^{PC}I_\varsigma$ represents the classical integral on $0 \le \varsigma \le \varsigma_0$ and the integral with exponential decay kernel on $\varsigma_1 \le \varsigma \le T$.

Definition 5. Let $\kappa(\varsigma)$ be differentiable function. The piecewise derivative [26] with classical derivative and the derivative with Mittag-Leffler kernel is given as

$$ {}_0^{PAB}D_\varsigma^\zeta \kappa(\varsigma) = \begin{cases} \kappa'(\varsigma) \text{ if } 0 \le \varsigma \le \varsigma_1 \\ {}_{\varsigma_1}^{AB}D_\varsigma^\zeta \kappa \ (\varsigma) \text{ if } \varsigma_1 \le \varsigma \le T \end{cases}, \tag{2.5} $$

where ${}_0^{PAB}D_\varsigma^\zeta$ represents the classical derivative on $0 \leq \varsigma \leq \varsigma_0$ and derivative with Mittag-Leffler kernel on $\varsigma_0 \leq \varsigma \leq T$.

Definition 6. The piecewise integral [26] with the classical integral and the integral formulation with the Mittag-Leffler kernel is expressed as:

$$ {}^{PAB}I_\varsigma \kappa\ (\varsigma) = \begin{cases} \int_0^\varsigma \kappa(\sigma)\, d\sigma \text{ if } 0 \leq \varsigma \leq \varsigma_1 \\ (1-\zeta)\,\kappa(\varsigma) + \frac{\zeta}{\Gamma(\zeta)} \int_{\varsigma_1}^\varsigma \kappa(\sigma)\,(\varsigma-\sigma)^{\zeta-1}\, d\sigma, \text{ if } \varsigma_1 \leq \varsigma \leq T \end{cases}, \tag{2.6} $$

where ${}^{PAB}I_\varsigma$ represents the classical integral on $0 \leq \varsigma \leq \varsigma_1$ and the integral with Mittag-Leffler kernel on $\varsigma_1 \leq \varsigma \leq T$.

The following formulas describe the fractional derivative with Mittag-Leffler kernel [25]

$$ {}_0^{ABC}D_\varsigma^\zeta \kappa(\varsigma) = \frac{1}{1-\zeta} \int_0^\varsigma \kappa'(\zeta)\, E_\zeta \left[-\frac{\zeta}{1-\zeta} (\varsigma-\sigma)^\zeta \right] d\sigma, \text{ in the Caputo sense} $$

and

$$ {}_0^{ABR}D_\varsigma^\zeta \kappa(\varsigma) = \frac{1}{1-\zeta} \frac{d}{d\varsigma} \int_0^\varsigma \kappa(\zeta)\, E_\zeta \left[-\frac{\zeta}{1-\zeta} (\varsigma-\sigma)^\zeta \right] d\sigma. \text{ in the Riemann-Liouville sense} $$

The corresponding integral is expressed as

$$ {}_0^{AB}J_\varsigma^\zeta \kappa(\varsigma) = (1-\zeta)\,\kappa(\varsigma) + \frac{\zeta}{\Gamma(\zeta)} \int_0^\varsigma \kappa(\zeta)\,(\varsigma-\sigma)^{\zeta-1}\, d\sigma. $$

3. Formulation of the Hepatitis C model

This section discusses deterministic and stochastic approaches for a Hepatitis C model presented in [18–20]. The equilibrium points and basic reproduction number will be analyzed for the deterministic model. Analyses such as numerical solutions, the existence and uniqueness of the solution of the model will be investigated for the stochastic model. In addition, the model will be modified using piecewise derivatives to capture crossover behaviors. This concept allows us to consider deterministic and stochastic frameworks for the Hepatitis C model. Models with deterministic-stochastic patterns will be numerically solved using the Newton polynomial approach.

3.1. Statement of the model for Hepatitis C

In this subsection, a mathematical model considering the spread of Hepatitis C virus will be discussed. The formulation of the model relies on a set of assumptions outlined in references [18–20]. In this framework, T, I, and V represent the populations of uninfected cells, infected cells, and free viral particles, respectively. Uninfected cells are supplied at a constant rate Λ and undergo natural degradation at rate δ_1. Viral infection occurs through contact between uninfected cells and free viruses at a transmission rate β, after which infected cells die at rate δ_2. The parameter η quantifies the drug's capacity to prevent viral entry into host cells, while ϵ measures its efficacy in suppressing viral replication. Infected cells produce hepatitis C virus at a steady rate k, and the free virus is eliminated from the system at a clearance rate c. The mathematical model under investigation is represented by:

$$ \begin{aligned} T'(t) &= \Lambda - \delta_1 T - (1-\eta)\,\beta V T, \\ I'(t) &= (1-\eta)\,\beta V T - \delta_2 I, \\ V'(t) &= (1-\epsilon)\,kI - cV. \end{aligned} \tag{3.1} $$

Initial conditions are as follows:

$$ T(0) = T_0 \geq 0,\ I(0) = I_0 \geq 0,\ V(0) = V_0 \geq 0. \tag{3.2} $$

3.2. Equilibrium points of the deterministic model

In this subsection, we present equilibrium points of the system by setting each equation of the system 3.1 equal to zero

$$\begin{aligned} \Lambda - \delta_1 T - (1-\eta)\,\beta V T &= 0, \\ (1-\eta)\,\beta V T - \delta_2 I &= 0, \\ (1-\epsilon)\,kI - cV &= 0. \end{aligned} \tag{3.3}$$

The disease-free equilibrium point is calculated as

$$E_0 = \left(\frac{\Lambda}{\delta_1}, 0, 0\right).$$

The endemic equilibrium point [19] is also found as

$$E_* = \left(\frac{\delta_2 c}{(1-\eta)\,(1-\epsilon)\,k\beta}, \frac{\Lambda}{\delta_2} - \frac{\delta_1 c}{(1-\eta)\,(1-\epsilon)\,k\beta}, \frac{(1-\epsilon)\,k\Lambda}{\delta_2 c} - \frac{\delta_1}{(1-\eta)\,\beta}\right). \tag{3.4}$$

3.3. Positivity of solutions in the deterministic model

In this subsection, we establish the positivity of the model's solutions under the assumption of positive initial conditions. To this perform, we begin by considering the function $V(t)$

$$V'(t) = (1-\epsilon)\,kI - cV, \tag{3.5}$$

which can be arranged as

$$V'(t) \geq -cV.$$

Then, the following inequality is achieved

$$V(t) \geq V(0)\,e^{-ct},$$

which proves the positivity of the function $V(t)$. Doing same routine for $I(t)$, we achieve

$$I'(t) \geq -\delta_2 I, \tag{3.6}$$

and

$$I(t) \geq I(0)\,e^{-\delta_2 t}.$$

For proof, we need to define the following norm

$$\|f\|_\infty = \sup_{t\in[0,T]} |f(t)|.$$

Now, we consider the function $T(t)$

$$\begin{aligned} T'(t) &\geq -\left(\delta_1 T + (1-\eta)\,\beta\,|V|\,T\right) \\ &\geq -\left(\delta_1 + (1-\eta)\,\beta \sup_{t\in[0,T]} |V|\right) \\ &\geq -\left(\delta_1 + (1-\eta)\,\beta\,\|V\|_\infty\right) T, \end{aligned} \tag{3.7}$$

and

$$T(t) \geq T(0)\,e^{-\left(\delta_1 + (1-\eta)\beta\|V\|_\infty\right)t}.$$

where $\eta < 1$.

3.4. Calculation of the basic reproduction number

In this subsection, the basic reproduction number is calculated for the Hepatitis C model employing the next generation matrix method [29]. To achieve our aim, we need to consider the infected classes of our model:

$$\begin{aligned} I'(t) &= (1-\eta)\beta VT - \delta_2 I, \\ V'(t) &= (1-\epsilon)kI - cV. \end{aligned} \tag{3.8}$$

The transition matrices are as follows:

$$JF = \begin{bmatrix} 0 & (1-\eta)\beta T \\ 0 & 0 \end{bmatrix},$$

and

$$JV = \begin{bmatrix} \delta_2 & 0 \\ -(1-\epsilon)k & c \end{bmatrix}.$$

By the help of the next generation method, we have

$$FV^{-1} = \begin{bmatrix} 0 & (1-\eta)\beta T \\ 0 & 0 \end{bmatrix} \begin{bmatrix} \frac{1}{\delta_2} & 0 \\ \frac{(1-\epsilon)k}{\delta_2 c} & \frac{1}{c} \end{bmatrix}, \tag{3.9}$$

and

$$FV^{-1} = \begin{bmatrix} \frac{(1-\eta)\beta T(1-\epsilon)k}{\delta_2 c} & \frac{(1-\eta)\beta T}{c} \\ 0 & 0 \end{bmatrix}.$$

The spectral radius of the matrix FV^{-1} leads to

$$R_0 = \frac{(1-\eta)\Lambda\beta(1-\epsilon)k}{\delta_1\delta_2 c}, \tag{3.10}$$

which is the reproduction number.

Here, it is concluded that the spread of the epidemic will increase if the basic reproduction number, that is, $R_0 > 1$, will increase, and if $R_0 < 1$, the spread of the virus will end [29].

4. Formulation of the stochastic Hepatitis C model

In this section, we aim to take a look at stochastic Hepatitis C model. We know that by adding stochastic noise to a deterministic system, the system can be generalized to stochastic processes. In the equation system below, $B_i(t)$, $i = 1, 2, 3$ is the standard Brownian motion, and σ_i, $i = 1, 2, 3$ is a real constant known as the density of noise. The mathematical model in question is represented by the following

$$\begin{aligned} dT(t) &= (\Lambda - \delta_1 T - (1-\eta)\beta VT)\,dt + \sigma_1 T(t)\,dB_1(t), \\ dI(t) &= ((1-\eta)\beta VT - \delta_2 I)\,dt + \sigma_2 I(t)\,dB_2(t), \\ dV(t) &= ((1-\epsilon)kI - cV)\,dt + \sigma_3 V(t)\,dB_3(t). \end{aligned} \tag{4.1}$$

4.1. Existence and uniqueness of the solutions

In this subsection, we will present the necessary properties for the existence and uniqueness of the solution of the stochastic Hepatitis C model given by (28). Before proceeding with the theorem, we denote the following notations

$$\psi = \begin{bmatrix} \psi_1 \\ \psi_2 \\ \psi_3 \end{bmatrix} = \begin{bmatrix} T \\ I \\ V \end{bmatrix}, \Omega(t,\psi) = \begin{bmatrix} \Omega_1(t,\psi) \\ \Omega_2(t,\psi) \\ \Omega_3(t,\psi) \end{bmatrix} = \begin{bmatrix} \Lambda - \delta_1 T - (1-\eta)\beta VT \\ (1-\eta)\beta VT - \delta_2 I \\ (1-\epsilon)kI - cV \end{bmatrix}.$$

Theorem 1. The solution of a stochastic differential equation, where $\Omega(t,\psi)$, is a function defined in Banach space, exists and is unique under the following conditions [30,31].

1. (Lipschitz condition) For $\forall\ \psi, \widetilde{\psi} \in H$ and $k_i > 0$

$$\left|\Omega_i\left(t,\psi\right)-\Omega_i\left(t,\widetilde{\psi}\right)\right|^2,\ \left|\Sigma_i\left(t,\psi\right)-\Sigma_i\left(t,\widetilde{\psi}\right)\right|^2 \leq k_i\left|\psi-\widetilde{\psi}\right|^2,\ \ t\geq 0.$$

2. (Linear growth condition) For $\forall\ \psi \in H$ and $\overline{k}_i > 0$

$$\left|\Omega_i\left(t,\psi\right)\right|^2,\ \left|\Sigma_i\left(t,\widetilde{\psi}\right)\right|^2 < \overline{k}_i\left(1+\left|\psi\right|^2\right),\ \ t\geq 0.$$

Proof. To prove the Lipschitz condition, we shall start the proof with first equation of the system

$$\begin{aligned}\left|\Omega_1\left(t,T\right)-\Omega_1\left(t,\widetilde{T}\right)\right|^2 &= \left|-\delta_1\left(T-\widetilde{T}\right)-\left(1-\eta\right)\beta V\left(T-\widetilde{T}\right)\right|^2 \\ &\leq 2\left(\delta_1^2+\left(1-\eta\right)^2\beta^2\left|V\right|^2\right)\left|T-\widetilde{T}\right|^2 \\ &\leq 2\left(\delta_1^2+\left(1-\eta\right)^2\beta^2\sup_{t\in[0,T]}\left|V\right|^2\right)\left|T-\widetilde{T}\right|^2 \\ &\leq 2\left(\delta_1^2+\left(1-\eta\right)^2\beta^2\left\|V\right\|_\infty^2\right)\left|T-\widetilde{T}\right|^2 \\ &\leq k_1\left|T-\widetilde{T}\right|^2,\end{aligned} \tag{4.2}$$

where

$$k_1 = 2\left(\delta_1^2+\left(1-\eta\right)^2\beta^2\left\|V\right\|_\infty^2\right).$$

For the proof of second equation of the system, we have

$$\begin{aligned}\left|\Omega_2\left(t,I\right)-\Omega_2\left(t,\widetilde{I}\right)\right|^2 &= \left|-\delta_2\left(I-\widetilde{I}\right)\right|^2 \\ &\leq \left(a_1+\delta_2^2\right)\left|I-\widetilde{I}\right|^2 \\ &\leq k_2\left|I-\widetilde{I}\right|^2,\end{aligned} \tag{4.3}$$

where

$$k_2 = a_1+\delta_2^2.$$

For the proof of last equation of the system, we obtain

$$\begin{aligned}\left|\Omega_3\left(t,V\right)-\Omega_3\left(t,\widetilde{V}\right)\right|^2 &= \left|-c\left(V-\widetilde{V}\right)\right|^2 \\ &\leq \left(a_2+c^2\right)\left|V-\widetilde{V}\right|^2 \\ &\leq k_3\left|V-\widetilde{V}\right|^2,\end{aligned} \tag{4.4}$$

where

$$k_2 = a_2+c^2.$$

For stochastic part, the following inequalities are valid:

$$\begin{aligned}\left|\Sigma_1\left(t,T\right)-\Sigma_1\left(t,\widetilde{T}\right)\right|^2 &= \sigma_1^2\left|T-\widetilde{T}\right|^2 \\ &\leq \left(a_3+\sigma_1^2\right)\left|T-\widetilde{T}\right|^2,\end{aligned} \tag{4.5}$$

$$\begin{aligned}\left|\Sigma_2(t,I)-\Sigma_2\left(t,\widetilde{I}\right)\right|^2 &= \sigma_2^2\left|I-\widetilde{I}\right|^2\\ &\leq \left(a_3+\sigma_2^2\right)\left|I-\widetilde{I}\right|^2,\end{aligned}$$

$$\begin{aligned}\left|\Sigma_3(t,V)-\Sigma_3\left(t,\widetilde{V}\right)\right|^2 &= \sigma_3^2\left|V-\widetilde{V}\right|^2\\ &\leq \left(a_3+\sigma_3^2\right)\left|V-\widetilde{V}\right|^2.\end{aligned}$$

Thus, we prove that the first condition of the Theorem 1 is verified. Now, we proceed with the proof of the second condition of Theorem 1.

$$\begin{aligned}|\Omega_1(t,T)|^2 &= |\Lambda-\delta_1 T-(1-\eta)\beta VT|^2\\ &\leq 3\left[\Lambda^2+\delta_1^2|T|^2+(1-\eta)^2\beta^2|V|^2|T|^2\right]\\ &\leq 3\left[\Lambda^2+\delta_1^2|T|^2+(1-\eta)^2\beta^2\sup_{0\leq t\leq T}|V|^2|T|^2\right]\\ &\leq 3\left[\Lambda^2+\left(\delta_1^2+(1-\eta)^2\beta^2\left\|V^2\right\|_\infty\right)|T|^2\right]\\ &\leq 3\Lambda^2\left(1+\frac{\delta_1^2+(1-\eta)^2\beta^2\left\|V^2\right\|_\infty}{\Lambda^2}|T|^2\right)\\ &\leq \overline{k}_1\left(1+\frac{\delta_1^2+(1-\eta)^2\beta^2\left\|V^2\right\|_\infty}{\Lambda^2}|T|^2\right),\end{aligned}$$

under the condition

$$\frac{\delta_1^2+(1-\eta)^2\beta^2\left\|V^2\right\|_\infty}{\Lambda^2}<1,$$

and $\overline{k}_1=3\Lambda^2$. Let us continue with the second equation of the system

$$\begin{aligned}|\Omega_2(t,I)|^2 &= |(1-\eta)\beta VT-\delta_2 I|^2\\ &\leq 2\left[(1-\eta)^2\beta^2\sup_{0\leq t\leq T}|V|^2\sup_{0\leq t\leq T}|T|^2+\delta_2^2|I|^2\right]\\ &\leq 2\left[(1-\eta)^2\beta^2\left\|V^2\right\|_\infty\left\|T^2\right\|_\infty+\delta_2^2|I|^2\right]\\ &\leq 2\left[(1-\eta)^2\beta^2\left\|V^2\right\|_\infty\left\|T^2\right\|_\infty\right]\left(1+\frac{\delta_2^2}{(1-\eta)^2\beta^2\left\|V^2\right\|_\infty\left\|T^2\right\|_\infty}|I|^2\right)\\ &\leq \overline{k}_2\left(1+\frac{\delta_2^2}{(1-\eta)^2\beta^2\left\|V^2\right\|_\infty\left\|T^2\right\|_\infty}|I|^2\right),\end{aligned}\tag{4.6}$$

under the condition

$$\frac{\delta_2^2}{(1-\eta)^2\beta^2\left\|V^2\right\|_\infty\left\|T^2\right\|_\infty}<1 \text{ and } \eta\neq 1,$$

and

$$\overline{k}_2=2\left[(1-\eta)^2\beta^2\left\|V^2\right\|_\infty\left\|T^2\right\|_\infty\right].$$

The following inequality is valid for the right-hand side function of the system in the third equation

$$\begin{aligned} |\Omega_3(t,V)|^2 &= |(1-\epsilon)kI - cV|^2 \\ &\leq 2\left[(1-\epsilon)^2 k^2 \sup_{0\leq t\leq T} |I|^2 + c^2 |I|^2\right] \\ &\leq 2\left[(1-\epsilon)^2 k^2 \left\|I^2\right\|_\infty + c^2 |I|^2\right] \\ &\leq 2\left[(1-\epsilon)^2 k^2 \left\|I^2\right\|_\infty\right]\left(1 + \frac{c^2}{(1-\epsilon)^2 k^2 \|I^2\|_\infty} |I|^2\right) \\ &\leq \overline{k}_3\left(1 + \frac{c^2}{(1-\epsilon)^2 k^2 \|I^2\|_\infty} |I|^2\right), \end{aligned} \tag{4.7}$$

under the condition

$$\frac{c^2}{(1-\epsilon)^2 k^2 \|I^2\|_\infty} < 1 \text{ and } \epsilon \neq 1,$$

and

$$\overline{k}_3 = 2\left[(1-\epsilon)^2 k^2 \left\|I^2\right\|_\infty\right].$$

Now, let us examine this condition for the functions $\Sigma_i(t,\psi)$

$$\begin{aligned} |\Sigma_1(t,T)|^2 &= \sigma_1^2 |T|^2 \\ &\leq \left(1+\sigma_1^2\right)|T|^2 \end{aligned} \tag{4.8}$$

$$\begin{aligned} |\Sigma_2(t,I)|^2 &= \sigma_2^2 |I|^2 \\ &\leq \left(1+\sigma_2^2\right)|I|^2 \end{aligned}$$

$$\begin{aligned} |\Sigma_3(t,V)|^2 &= \sigma_3^2 |V|^2 \\ &\leq \left(1+\sigma_3^2\right)|V|^2. \end{aligned}$$

Therefore, it is concluded that the solution of the stochastic model exists and is unique under the condition

$$\max\left\{\frac{\delta_1^2 + (1-\eta)^2\beta^2\left\|V^2\right\|_\infty}{\Lambda^2}, \frac{\delta_2^2}{(1-\eta)^2\beta^2\|V^2\|_\infty\|T^2\|_\infty}, \frac{c^2}{(1-\epsilon)^2 k^2 \|I^2\|_\infty}\right\} < 1. \tag{4.9}$$

5. Piecewise Hepatitis C model with different patterns: Classical, fractional and stochastic

In this section, we examine various formulations of the Hepatitis C model in which piecewise derivatives are applied. Depending on the scenario, the model may involve deterministic dynamics in the first interval and stochastic dynamics in the second; in some cases, the Atangana–Baleanu derivative is used, while in others, Caputo-Fabrizio or Caputo-type stochastic derivatives are employed. To numerically solve these formulations, we construct a method based on Newton polynomial interpolation [23].

5.1. Deterministic Hepatitis C model with piecewise setting: Classical- Atangana-Baleanu- Caputo fractional derivative

In this subsection, we deal with a piecewise Hepatitis C model composed of three distinct intervals: the first interval follows a deterministic structure, the second incorporates the Caputo fractional derivative, and

the third employs the Atangana–Baleanu fractional derivative. The mathematical formulation of the model under investigation is given by:

$$\begin{cases} \psi'(t) = \Omega(t,\psi),\ 0 \le t \le t_0 \\ {}_{t_0}^{C}D_t^{\zeta}\psi(t) = \Omega(t,\psi), t_0 \le t \le t_1 \\ {}_{t_1}^{AB}D_t^{\zeta}\psi(t) = \Omega(t,\psi),\ t_1 \le t \le T \end{cases}. \tag{5.1}$$

Integrating above, we have

$$\psi(t) = \begin{cases} \psi(0) + \int_0^t \Omega(\sigma,\psi)\, d\sigma, 0 \le t \le t_0 \\ \psi(t_0) + \dfrac{1}{\Gamma(\zeta)} \int_{t_0}^t \Omega(\sigma,\psi)(t-\sigma)^{\zeta-1} d\sigma, t_0 \le t \le t_1 \\ \psi(t_1) + (1-\zeta)\Omega(t,\psi) + \dfrac{\zeta}{\Gamma(\zeta)} \int_{t_1}^t \Omega(\sigma,\psi)(t-\sigma)^{\zeta-1} d\sigma, t_1 \le t \le T \end{cases}, \ . \tag{5.2}$$

The numerical algorithm obtained by solving the piecewise model using a Newton polynomial-based method [23] is formulated as follows:

$$\psi^{\gamma+1} = \begin{cases} \left\{ \psi(t_0) + h\sum_{\xi=m+3}^{\xi_1} \begin{bmatrix} \frac{23}{12}\Omega\left(t_\xi,\psi^\xi\right) - \frac{4}{3}\Omega\left(t_{\xi-1},\psi^{\xi-1}\right) \\ +\frac{5}{12}\Omega\left(t_{\xi-2},\psi^{\xi-2}\right) \end{bmatrix},\ 0 \le t \le t_0 \right. \\ \begin{cases} \psi(t_0) + \dfrac{h^\zeta}{\Gamma(\zeta+2)} \sum_{\xi=\xi_1+1}^{\xi_2} \Omega\left(t_{\xi-2},\psi^{\xi-2}\right) \Pi_{\xi_2,\xi}^1 \\ + \dfrac{h^\zeta}{\Gamma(\zeta+2)} \sum_{\xi=\xi_1+1}^{\xi_2} \left[\Omega\left(t_{\xi-1},\psi^{\xi-1}\right) - \Omega\left(t_{\xi-2},\psi^{\xi-2}\right)\right] \Pi_{\xi_2,\xi}^2 \\ + \dfrac{h^\zeta}{\Gamma(\zeta+3)} \sum_{\xi=\xi_1+1}^{\xi_2} \begin{bmatrix} \Omega\left(t_\xi,\psi^\xi\right) - 2\Omega\left(t_{\xi-1},\psi^{\xi-1}\right) \\ +\Omega\left(t_{\xi-2},\psi^{\xi-2}\right) \end{bmatrix} \Pi_{\xi_2,\xi}^3, 0 \le t \le t_0, \end{cases}, t_0 \le t \le t_1 \\ \begin{cases} \psi(t_1) + (1-\zeta)\Omega\left(t_\gamma,\psi^\gamma\right) \\ + \dfrac{\zeta h^\zeta}{\Gamma(\zeta+2)} \sum_{\xi=\xi_2+1}^{\gamma} \Omega\left(t_{\xi-2},\psi^{\xi-2}\right) \Pi_{\gamma,\xi}^1 \\ + \dfrac{\zeta h^\zeta}{\Gamma(\zeta+2)} \sum_{\xi=\xi_2+1}^{\gamma} \left[\Omega\left(t_{\xi-1},\psi^{\xi-1}\right) - \Omega\left(t_{\xi-2},\psi^{\xi-2}\right)\right] \Pi_{\gamma,\xi}^2 \\ + \dfrac{\zeta h^\zeta}{\Gamma(\zeta+3)} \sum_{\xi=\xi_2+1}^{\gamma} \begin{bmatrix} \Omega\left(t_\xi,\psi^\xi\right) - 2\Omega\left(t_{\xi-1},\psi^{\xi-1}\right) \\ +\Omega\left(t_{\xi-2},\psi^{\xi-2}\right) \end{bmatrix} \Pi_{\gamma,\xi}^3, 0 \le t \le t_0, \end{cases}, t_1 \le t \le T \end{cases}, \tag{5.3}$$

where

$$\begin{aligned} \Pi_{\xi_2,\xi}^1 &= \left[(\xi_2-\xi+1)^\zeta - (\xi_2-\xi)^\zeta\right], \\ \Pi_{\xi_2,\xi}^2 &= \begin{bmatrix} (\xi_2-\xi+1)^\zeta(\xi_2-\xi+3+2\zeta) \\ -(\xi_2-\xi)^\zeta(\xi_2-\xi+3+3\zeta) \end{bmatrix}, \\ \Pi_{\xi_2,\xi}^3 &= \begin{bmatrix} (\xi_2-\xi+1)^\zeta \begin{bmatrix} 2(\xi_2-\xi)^2 + (3\zeta+10)(\xi_2-\xi) \\ +2\zeta^2+9\zeta+12 \end{bmatrix} \\ -(\xi_2-\xi)^\zeta \begin{bmatrix} 2(\xi_2-\xi)^2 + (5\zeta+10)(\xi_2-\xi) \\ +6\zeta^2+18\zeta+12 \end{bmatrix} \end{bmatrix}. \end{aligned} \tag{5.4}$$

Figures 1–3 illustrate the numerical simulations for each class of the piecewise model: the first segment employs the classical derivative, the second utilizes the Caputo fractional derivative, and the third incorporates the Atangana–Baleanu fractional derivative.

The numerical simulations presented in Figures 1–3 illustrate the dynamic behavior of a piecewise fractional-order model for hepatitis infection. The figures demonstrate how varying the fractional-order parameter ζ significantly influences the system's dynamics. When $\zeta = 1$, corresponding to the classical derivative, the solutions exhibit rapid transitions with smooth decays. However, as ζ decreases—indicating

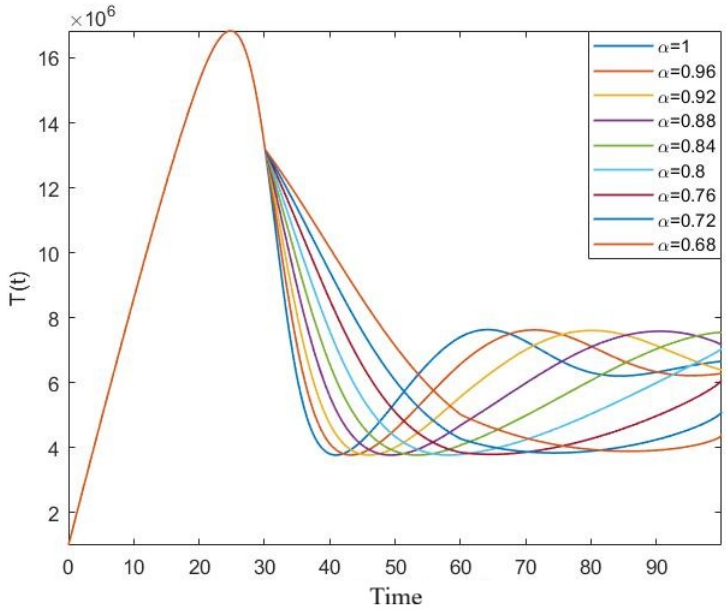

Figure 1: Dynamics of the uninfected population class within the piecewise differential framework for various values of α.

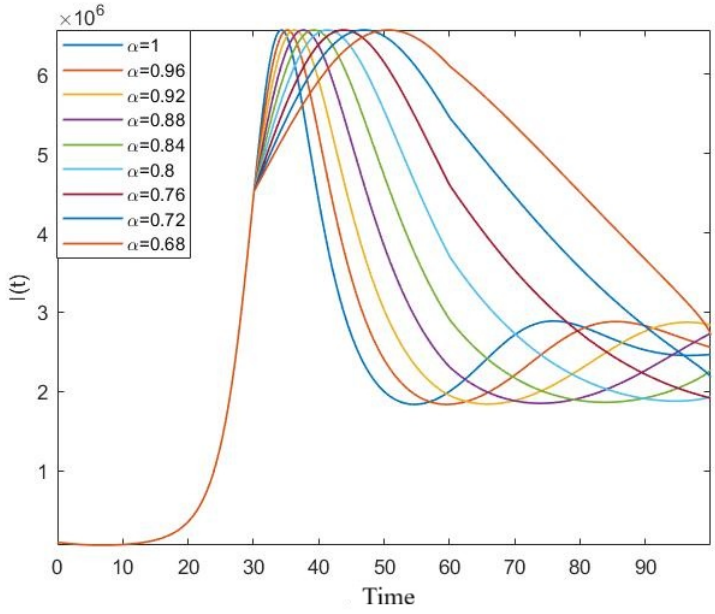

Figure 2: Evolution of the infected population class modeled using a piecewise differential approach for different values of α.

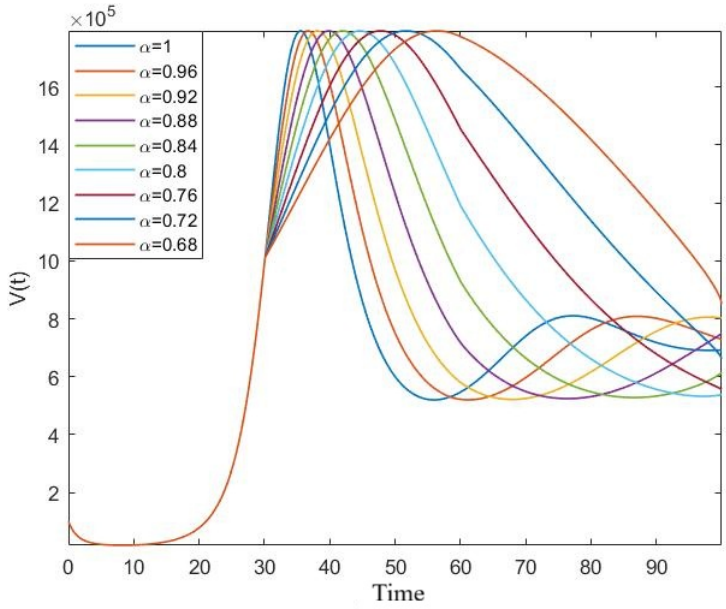

Figure 3: Dynamics of the free virus class within a piecewise differential framework for varying values of α.

the incorporation of memory effects through fractional calculus—the system displays more complex behaviors, including delayed responses, oscillations, and slower convergence to equilibrium. These effects are particularly evident in the second and third segments of the piecewise model, where Caputo and Atangana–Baleanu fractional derivatives are employed. The presence of these oscillations and prolonged decay phases aligns with biological observations in hepatitis dynamics, where immune response and viral replication can exhibit time-dependent and history-sensitive patterns. Overall, the results highlight the importance of fractional modeling in capturing the memory and hereditary characteristics inherent in biological systems.

5.2. Deterministic-stochastic Hepatitis C model with piecewise setting: Stochastic- Caputo-Fabrizio fractional derivative

In this subsection, a piecewise Hepatitis C model is considered, in which the first interval is governed by a deterministic structure, while the second interval is characterized by stochastic dynamics described using the Caputo-Fabrizio fractional derivative. The mathematical formulation of the model under investigation is given by:

$$\begin{cases} d\psi(t) = \Omega(t,\psi)\,dt + \sigma_i \psi dB_i(t), \ 0 \le t \le t_0 \\ {}^{C\Omega}_{t_0}D^{\zeta}_{t}\psi(t) = \Omega(t,\psi), t_0 \le t \le T \end{cases}. \tag{5.5}$$

Performing the piecewise integration above leads to

$$\psi(t) = \begin{cases} \psi(0) + \int_0^t \Omega(\sigma,\psi)\,d\sigma + \sigma_i \int_0^t \psi(\sigma)\,dB_i(\sigma), 0 \le t \le t_0 \\ \psi(t_0) + (1-\zeta)\,\Omega(t,\psi) + \zeta \int_{t_0}^t \Omega(\sigma,\psi)\,d\sigma, t_0 \le t \le T \end{cases}. \tag{5.6}$$

The piecewise model solution, obtained through a Newton polynomial-based approach [23], is formulated numerically as:

$$\psi^{\gamma+1} = \begin{cases} \begin{cases} \psi^{\gamma} + h \left[\begin{array}{c} \frac{23}{12}\Omega(t_\gamma,\psi^\gamma) - \frac{4}{3}\Omega\left(t_{\gamma-1},\psi^{\gamma-1}\right) \\ +\frac{5}{12}\Omega\left(t_{\gamma-2},\psi^{\gamma-2}\right) \end{array} \right] \\ +\sum_{k=0}^{\gamma} \sigma_i \psi(c_k)\left(B_i(t_{k+1}) - B_i(t_k)\right), \ 0 \le t \le t_0 \end{cases} \\ \begin{cases} \psi^{\gamma} + (1-\zeta)\,\Omega(t_\gamma,\psi^\gamma) \\ +\zeta h \left[\begin{array}{c} \frac{23}{12}\Omega(t_\gamma,\psi^\gamma) - \frac{4}{3}\Omega\left(t_{\gamma-1},\psi^{\gamma-1}\right) \\ +\frac{5}{12}\Omega\left(t_{\gamma-2},\psi^{\gamma-2}\right) \end{array} \right] \end{cases}, t_0 \le t \le T \end{cases}, \tag{5.7}$$

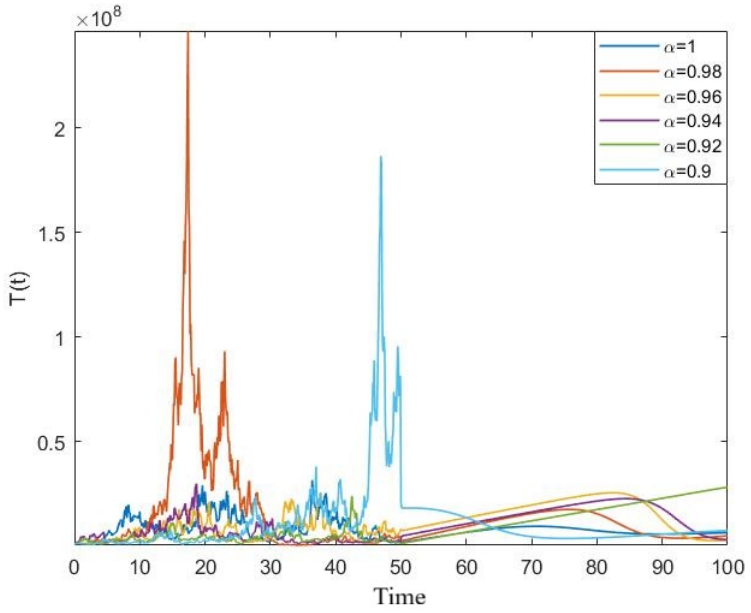

Figure 4: Graphical representation of the uninfected class dynamics using a piecewise differential formulation for a range of α values.

where $c_k \in [t_k, t_{k+1}]$.

In Figure 4-6, the numerical simulations are depicted for each class of piecewise model with stochastic and Caputo-Fabrizio fractional derivative where the stochastic constants are taken as $\sigma_1 = 0.18$, $\sigma_1 = 0.16$ and $\sigma_1 = 0.21$.

Figures 4-6 depict the evolution of uninfected cells $T(t)$, infected cells $I(t)$, and free virus particles $V(t)$, respectively, for various values of the fractional-order parameter ζ. In Figure 4, the dynamics of $T(t)$ reveal significant irregularity and noise-induced oscillations, particularly for higher ζ values such as $\zeta = 1$ and $\zeta = 0.98$, where sudden spikes and instability are observed. These fluctuations are indicative of the system's sensitivity to random disturbances under weaker memory effects. As ζ decreases, the model exhibits more damped and stable trajectories, suggesting that stronger memory effects inherent to fractional operators can mitigate the influence of stochasticity over time. Similarly, Figure 5 shows that the number of infected cells $I(t)$ increases sharply for larger ζ values, resulting in pronounced peaks followed by rapid declines. This behavior reflects the system's susceptibility to rapid viral spread and immune response in low-memory (higher-ζ) regimes. However, for lower ζ values, such as 0.92 and 0.9, the dynamics become smoother and more sustained, indicating that fractional memory helps distribute the infection dynamics over a longer time horizon, reducing abrupt transitions. In Figure 6, the dynamics of the viral load $V(t)$ follow a similar trend. High ζ values result in large, noisy fluctuations in viral concentration, with sharp peaks resembling sudden viral bursts. In contrast, lower ζ values lead to smoother, more regular oscillations that stabilize over time.

5.3. Deterministic-stochastic Hepatitis C model with piecewise setting: Classical- stochastic Caputo fractional derivative

In this subsection, we consider a piecewise Hepatitis C model in which the first interval follows a deterministic structure, while the second interval incorporates stochastic dynamics. The mathematical formulation of the model under investigation is given by:

$$\begin{cases} \psi'(t) = \Omega(t, \psi), \ 0 \le t \le t_0 \\ {}^{C}_{t_0}D^{\zeta}_{t}\psi(t) = \Omega(t, \psi) + \sigma_i \psi B_i'(t), t_0 \le t \le T \end{cases}. \tag{5.8}$$

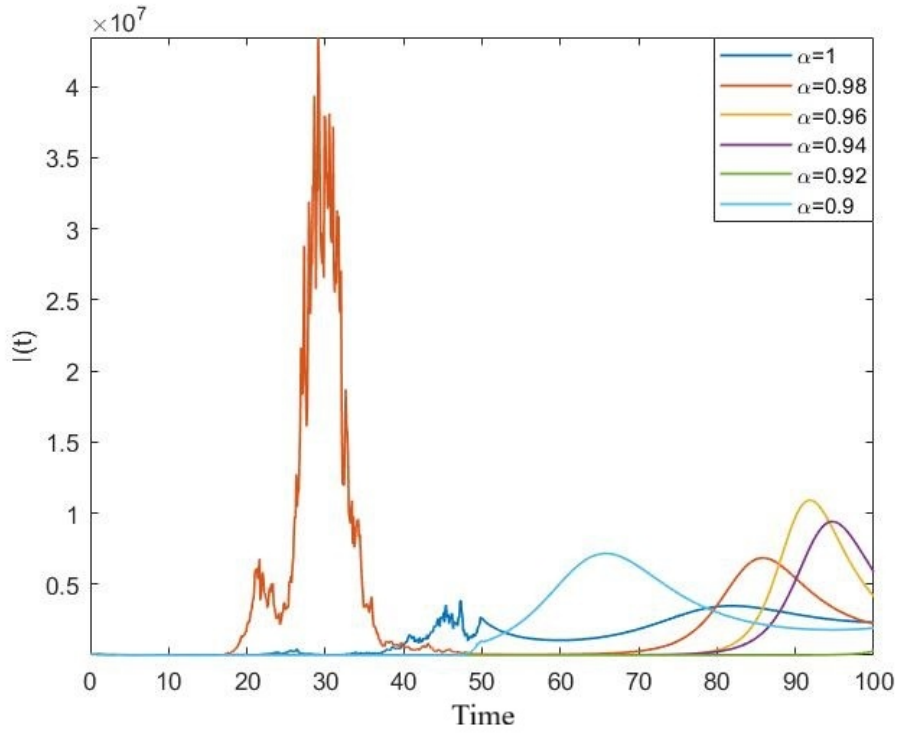

Figure 5: Visualization of infected class evolution governed by a piecewise differential approach across selected α values.

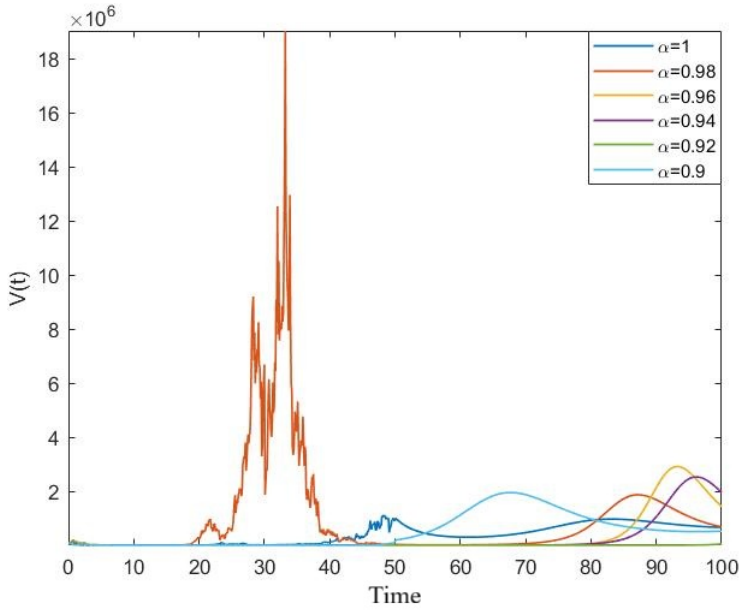

Figure 6: Representation of the free virus population dynamics using a piecewise stochastic model incorporating classical and Caputo derivatives under varying α values.

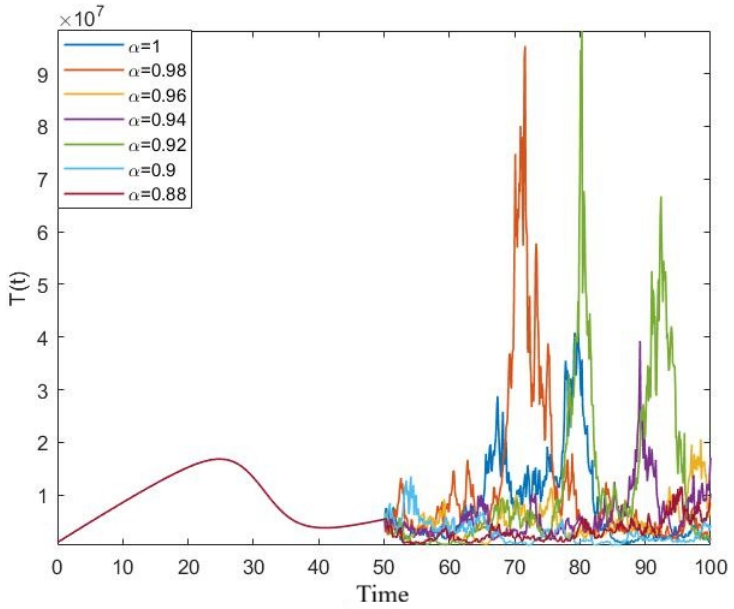

Figure 7: Piecewise stochastic representation of the uninfected class dynamics using classical and Caputo derivatives under varying α values.

Upon integrating the above system, we obtain

$$\psi(t)=\begin{cases}\psi(0)+\int_0^t\Omega(\sigma,\psi)\,d\sigma, 0\le t\le t_0\\ \psi(t_0)+\dfrac{1}{\Gamma(\zeta)}\int_{t_0}^t\Omega(\sigma,\psi)(t-\sigma)^{\zeta-1}d\sigma+\sigma_i\int_{t_0}^t\psi(\sigma)\,dB_i(\sigma), t_0\le t\le T\end{cases}. \tag{5.9}$$

Using the Newton polynomial method to solve the piecewise model, the resulting numerical algorithm can be stated as:

$$\psi^{\gamma+1}=\begin{cases}\left\{\psi(t_0)+h\sum_{\xi=m+3}^{\xi_1}\left[\begin{array}{c}\frac{23}{12}\Omega\left(t_\xi,\psi^\xi\right)-\frac{4}{3}\Omega\left(t_{\xi-1},\psi^{\xi-1}\right)\\+\frac{5}{12}\Omega\left(t_{\xi-2},\psi^{\xi-2}\right)\end{array}\right], 0\le t\le t_0\\ \left\{\begin{array}{c}\psi(t_0)+\dfrac{h^\zeta}{\Gamma(\zeta+2)}\sum_{\xi=\xi_1+1}^{\xi_2}\Omega\left(t_{\xi-2},\psi^{\xi-2}\right)\Pi^1_{\xi_2,\xi}\\ +\dfrac{h^\zeta}{\Gamma(\zeta+2)}\sum_{\xi=\xi_1+1}^{\xi_2}\left[\Omega\left(t_{\xi-1},\psi^{\xi-1}\right)-\Omega\left(t_{\xi-2},\psi^{\xi-2}\right)\right]\Pi^2_{\xi_2,\xi}\\ +\dfrac{h^\zeta}{\Gamma(\zeta+3)}\sum_{\xi=\xi_1+1}^{\xi_2}\left[\begin{array}{c}\Omega\left(t_\xi,\psi^\xi\right)-2\Omega\left(t_{\xi-1},\psi^{\xi-1}\right)\\+\Omega\left(t_{\xi-2},\psi^{\xi-2}\right)\end{array}\right]\Pi^3_{\xi_2,\xi}\\ +\sum_{k=0}^{\gamma}\sigma_i\psi(c_k)\left(B_i(t_{k+1})-B_i(t_k)\right)\end{array}, t_0\le t\le T\end{cases}. \tag{5.10}$$

In Figure 7-9, the numerical simulations for the piecewise model with classical and Caputo stochastic are performed for each class of model where the stochastic constants are taken as $\sigma_1=0.18$, $\sigma_1=0.16$ and $\sigma_1=0.21$.

The numerical results corresponding to this model are illustrated in Figures 7-9, where the dynamics of uninfected cells $T(t)$, infected cells $I(t)$, and free virus particles $V(t)$ are shown for different values of the fractional-order parameter ζ. The stochasticity introduced in the second interval results in high variability, particularly for larger ζ values such as $\zeta=1$ and $\zeta=0.98$, where the trajectories exhibit significant noise and abrupt spikes. For instance, Figure 7 displays sharp and irregular fluctuations in the number of uninfected cells, especially for $\zeta=0.98$, reflecting how sensitive the system becomes under low-memory stochastic regimes. A similar trend is observed in Figure 8, where the number of infected cells rapidly escalates and then drops off sharply for higher ζ, suggesting intense but short-lived infection waves.

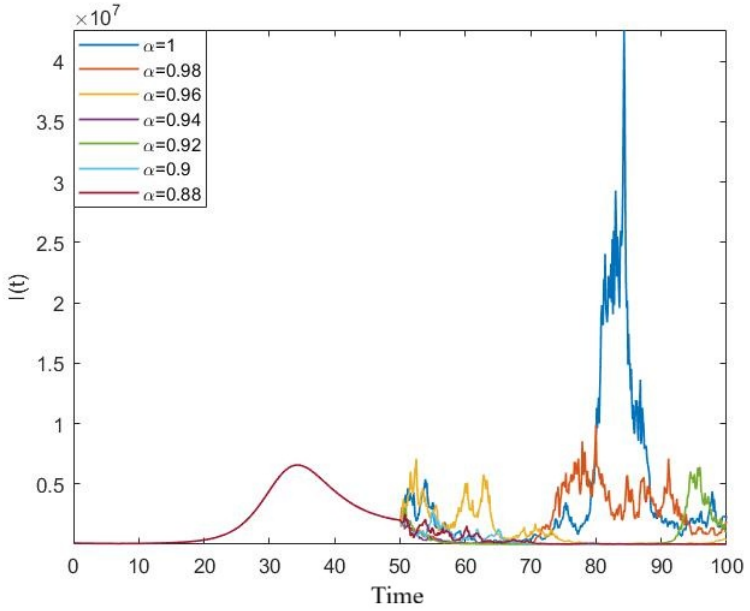

Figure 8: Infected class dynamics captured via a piecewise stochastic framework employing classical and Caputo operators for varying α parameters.

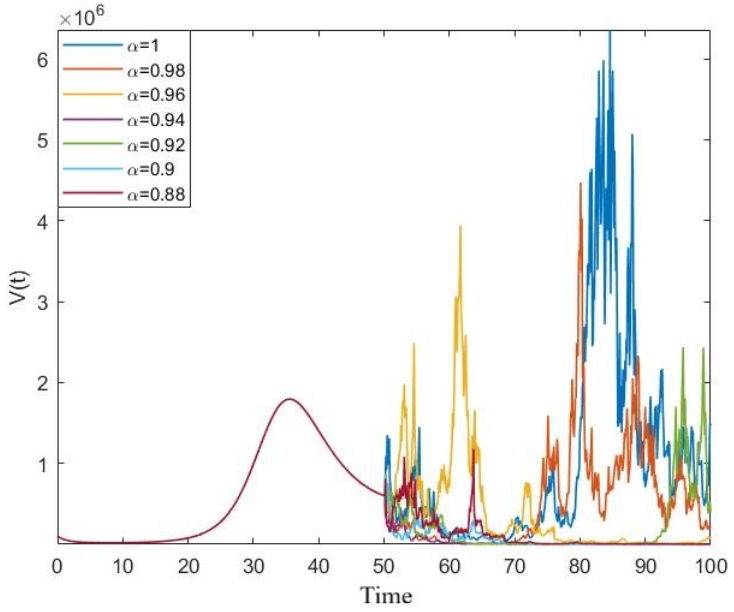

Figure 9: Representation of the behavior of the free virus population using a piecewise stochastic model with classical and Caputo derivatives under varying α values.

In contrast, as ζ decreases (e.g., $\zeta = 0.92$ or $\zeta = 0.9$), the system exhibits more gradual and smoothed responses, with oscillatory yet stable patterns that indicate a damping effect from the memory property of the Caputo derivative. Figure 9 further confirms this, showing viral load dynamics that become less erratic and more predictable with decreasing ζ. Overall, the results demonstrate that incorporating fractional-order memory and stochasticity offers a more flexible and realistic representation of hepatitis C infection dynamics, capturing both sudden shifts and long-term regulatory behavior.

6. Conclusion

This study presents a comprehensive investigation of a Hepatitis C virus (HCV) transmission model that integrates both classical (integer-order) and fractional (non-integer-order) derivatives within deterministic and stochastic frameworks. To numerically approximate the solutions of the model's differential equations, a Newton polynomial interpolation-based method is employed. In the deterministic setting, the model is analyzed with respect to equilibrium points, the basic reproduction number, and the positivity of solutions. For the stochastic case, the existence and uniqueness of solutions are established, and a tailored numerical algorithm is developed and implemented accordingly. The model is further extended using the concept of piecewise differential operators introduced by Atangana and Araz, enabling a unified framework that captures both deterministic and stochastic behaviors across different time intervals. These operators offer a powerful mathematical tool to model systems undergoing transitions between dynamic regimes—something traditional operators fail to address adequately. Prior to their introduction, existing methods lacked the structural flexibility to coherently integrate stochasticity and memory effects within a single modeling approach.

Graphical simulations of the model under piecewise dynamics—particularly with stochastic Caputo fractional operators—highlight the emergence of behaviors not observable in purely classical or standard fractional models. The numerical results show that higher fractional orders (ζ close to 1) lead to greater stochastic variability and abrupt fluctuations, while lower orders smooth out these irregularities, reflecting the stabilizing influence of memory. These effects are clearly evident in the oscillatory patterns and delayed transitions of uninfected, infected, and viral populations across different ζ values. This behavior aligns more closely with real-world biological complexity, where disease progression and immune response often exhibit both randomness and historical dependence.

Overall, the application of piecewise fractional operators in this context bridges a critical gap in infectious disease modeling. By allowing the coexistence of deterministic precision and stochastic variability within a single framework, this approach significantly enhances the realism and flexibility of mathematical models, offering valuable insights into the dynamics of Hepatitis C and potentially other infectious diseases.

References

[1] Dietz, C., Maasoumy, B., 2022. *Direct-acting antiviral agents for hepatitis C virus infection—From drug discovery to successful implementation in clinical practice.* Viruses, **14 (6)**, 1325.

[2] Feinstone, S.M., Kapikian, A.Z., Purcell, R.H., Alter, H.J., Holland, P.V., 1975. *Transfusion-associated hepatitis not due to viral hepatitis type A or B.* New England Journal of Medicine, **292 (15)**, 767-770.

[3] Choo, Q.L., Kuo, G., Weiner, A.J., Overby, L.R., Bradley, D.W., Houghton, M., 1989. *Isolation of a cDNA clone derived from a blood-borne non-A, non-B viral hepatitis genome.* Science, **244**, 359–362.

[4] Kuo, G., Choo, Q.L., Alter, H.J., Gitnick, G.L., Redeker, A.G., Purcell, R.H., Miyamura, T., Dienstag, J.L., Alter, M.J., Stevens, C.E., Tegtmeier, G.E., Bonino, M., Lee, W.S., Kuo, C., Berger, K., Shuster, J.R., Overby, L.R., Bradley, D.W., Houghton, M., 1989. *An assay for circulating antibodies to a major etiologic virus of human non-A, non-B hepatitis.* Science, **244**, 362–366.

[5] Sadki, M., Danane, J., Allali, K., 2023. *Hepatitis C virus fractional-order model: Mathematical Analysis.* Modeling Earth Systems and Environment, **9 (2)**, 1695-1707.

[6] Maasoumy, B., Wedemeyer, H., 2012. *Natural history of acute and chronic hepatitis C. Best practice & research Clinical gastroenterology*, **26 (4)**, 401-412.

[7] Collaborators, H., 2017. *Global prevalence and genotype distribution of hepatitis C virus infection in 2015: A modelling study.* Lancet Gastroenterol. Hepatol. **2**, 161–176.

[8] Duncan, J.D., Urbanowicz, R.A., Tarr, A.W., Ball, J.K., 2020. *Hepatitis C virus vaccine: Vhallenges and prospects.* Vaccines, **8 (1)**, 90.
[9] Larney, S., Peacock, A., Leung, J., Colledge, S., Hickman, M., Vickerman, P., Grebely, J., Dumchev, K.V., Griffiths, P., Hines, L., Cunningham E.B., Mattick R.P., Lynskey M., Marsden J., Strang J., Degenhardt L., 2017. *Global, regional, and country-level coverage of interventions to prevent and manage HIV and hepatitis C among people who inject drugs: A systematic review.* Lancet Glob. Health, **5**, 1208–1220. 1
[10] Dayan, F., Ahmed N., Bariq A., Akgül A., Jawaz M., Rafiq M., Raza A., *Computational study of a co-infection model of HIV/AIDS and hepatitis C virus models*, Scientific Reports, **13(1)**, 2023.
[11] Pitcher AB, Borquez A, Skaathun B, Martin NK. *Mathematical modeling of Hepatitis C virus (HCV) prevention among people who inject drugs: A review of the literature and insights for elimination strategies.* J Theor Biol. 2019, **21**;481:194-201. 1
[12] Dahari H., Ribeiro RM., Rice CM., Perelson AS., *Mathematical Modeling of Subgenomic Hepatitis C Virus Replication in Huh-7 Cells*, 2007, Journal of Virology, **81 (2)**, 750-760. 1
[13] Deebani W., Jan R., Shah Z., Vrinceanu N, Racheriu M., 2023. *Modeling the transmission phenomena of water-borne disease with non-singular and non-local kernel*, Comput Methods Biomech Biomed Engin., **26 (11)**, 1294-1307.
[14] Tang TQ., Jan R., Rehman Z., Shah Z., Vrinceanu N., Racheriu M., 2022. *Modeling the dynamics of chronic myelogenous leukemia through fractional calculus*, Fractals, **30 (10)**.
[15] Sultan A., Jan R., 2023. *Qualitative and Quantitative Analysis of Fractional Dynamics of Infectious Diseases with Control Measures*, Fractal and Fractional, **7 (5)**, 400.
[16] Zafar AA., Sadiq MA., Shabbir K., Guran L., *A computational study of vibrating system using the constant proportional Caputo derivative operator approach*, International Journal of Modern Physics C (IJMPC), **36 (5)**, 2025, 1-31.
[17] Vujovic, V., Krstic, M., 2020. *Stability of Stochastic Model for Hepatitis-C Transmission with an Isolation stage*, Filomat, **34 (14)**, 4795–4809. 1
[18] Lestari, D., Adi-Kusumo, F., Megawati, N. Y., Susyanto, N. 2023. *A minimum principle for stochastic control of hepatitis C epidemic model.* Boundary Value Problems, **2023 (1)**, 1-12, 2023. 1
[19] Lestari, D., Megawati, N. Y., Susyanto, N., Adi-Kusumo, F., 2022. *Qualitative behaviour of a stochastic hepatitis C epidemic model in cellular level,* Mathematical Biosciences and Engineering, **19**, 1515-1535. 1, 3.2
[20] Topuz, C., 2021. *Parameter estimation for stochastic differential equations*, Dissertation, Ankara University, 33-34. 1
[21] Caputo M., *Linear model of dissipation whoseQ is almost frequency independent.* II. Geophysical Journal International, **13 (5)**: 1967, 529-539. 1
[22] Podlubny I., *Fractional differential equations, vol. 198 of Mathematics in Science and Engineering*, Academic Press, San Diego, 1999, ISBN: 9780125588409. 1
[23] Atangana, A., İğret Araz, S., 2021. *New numerical scheme with Newton polynomial: Theory, methods and applications*, Elsevier, Academic press, ISBN:9780323854481. 1, 5, 5.1, 5.2
[24] Caputo, M., Fabrizio, M., 2015. *A new definition of fractional derivative without singular kernel.* Progress in Fractional Differentiation & Applications, **1 (2)**, 73-85. 1, 2
[25] Atangana, A., Baleanu, D., 2016. *New fractional derivatives with non-local and non-singular kernel: Theory and application to heat transfer model,* Thermal Science, **20 (2)**, 763-769. 1, 2
[26] Atangana, A., İğret Araz, S., 2021. *New concept in calculus: Piecewise differential and integral operators*, Chaos, Solitons and Fractals, 145. 1, 2, 2, 2, 2
[27] Boulaaras S., Igret Araz S., Alharbi A., Radiotherapy Effects in Tumor Treatment: A Piecewise Model with Deterministic and Stochastic Approaches, Fractals, 2025. 1
[28] Cetin MA., Igret Araz S., Prediction of COVID-19 spread with models in different patterns: A case study of Russia, Open Physics, **22 (1)**, 2024. 1
[29] Driessche, P.V., Watmough, J., 2002. *Reproduction numbers and sub-threshold endemic equilibria for compartmental models of disease transmission,* Mathematical Biosciences, **180 (1-2)**, 29-48. 3.4, 3.4
[30] Steele, M.J., *Stochastic Calculus and Financial Applications*, Springer, 2010.
[31] Atangana, A., İğret Araz, S., *Fractional stochastic differential equations applications to Covid-19 modeling*, Springer, 2022.